# HIGH ACETYLCHOLINE CONCENTRATIONS CAUSE RAPID INACTIVATION BEFORE FAST DESENSITIZATION IN NICOTINIC ACETYLCHOLINE RECEPTORS FROM *TORPEDO*

STUART A. FORMAN* AND KEITH W. MILLER‡
*Committee on Higher Degrees in Biophysics, Harvard University, Cambridge, Massachusetts 02139; *Program in Health Sciences and Technology, Massachusetts Institute of Technology, Cambridge, Massachusetts 02142; ‡Department of Pharmacology, Harvard Medical School, Boston, Massachusetts 02115; and ‡Department of Anesthesia, Massachusetts General Hospital, Boston, Massachusetts 02114

ABSTRACT By using both a 3 to 4 ms quenched-$^{86}Rb^+$ flux assay and native acetylcholine receptor (AChR) rich electroplaque vesicles on which 50–60% of acetylcholine activation sites were blocked with $\alpha$-BTX, we determined apparent rates of agonist-induced inactivation in AChR from *Torpedo* under conditions where measured flux response was directly proportional to initial $^{86}Rb^+$ influx rate. Inactivation kinetics with acetylcholine in both the activating range (10 $\mu$M–10 mM) and the self-inhibiting range (15–100 mM) were measured at 4°C. In the presence of 10 $\mu$M–1 mM acetylcholine, inactivation is characterized by a single exponential rate constant, $k_d$ (fast desensitization). Plots of $k_d$ vs. acetylcholine concentration display maximum $k_d$s [$k_d$(max)] of 6.6–8.0 $s^{-1}$, half-maximal $k_d$ at 102 ± 16 $\mu$M, and a Hill coefficient of 1.6 ± 0.3, closely paralleling the initial ion flux response of AChR. Thus, fast desensitization probably occurs from a doubly-liganded preopen state or the open channel state. In the self-inhibiting acetylcholine concentration range, inactivation is biphasic. A "rapid inactivation" phase is complete within 30 ms, followed by fast desensitization at a rate close to $k_d$(max). Both the rate and extent of rapid inactivation increase with acetylcholine concentration, indicating that acetylcholine binds to its self-inhibition site with apparent $k_{on} \simeq 10^3$ $M^{-1}s^{-1}$ and $k_{off} \simeq 40$ $s^{-1}$. This slow $k_{on}$ suggests either hindered access to the inhibitory allosteric site or that a fast binding step is followed by a slower conformational change leading to channel inhibition. Overall, our data suggest that acetylcholine binds preferentially to its inhibitory site when the receptor is in the open-channel conformation and that fast desensitization can occur from all muliple-liganded states.

## INTRODUCTION

Depolarization of the motor endplate by acetylcholine (ACh)[1] is mediated by a five-subunit protein complex, the nicotinic acetylcholine receptor (AChR), which contains binding sites for ACh and a cation selective transmembrane channel. In addition to stimulating AChR channel opening, ACh inactivates channel function by three different mechanisms. Over increasing ACh concentration ranges, these inactivation processes are termed slow desensitization (seconds to minute time scale), fast desensitization (milliseconds to seconds), and self inhibition (for reviews see Changeux et al., 1984 and Udgaonkar and Hess, 1986). Slow and fast desensitization are thought to be triggered by agonist binding to receptor sites (Katz and Thesleff, 1957; but see Dunn and Raftery, 1982), whereas self inhibition is thought to occur by either a channel blocking mechanism (Sine and Steinbach, 1984) or an allosteric site mechanism (Pasquale et al., 1983; Takeyasu et al., 1986).

In vitro studies of both ligand binding and rapid tracer ion flux techniques in AChR-rich membrane vesicles from electroplaque tissue of *Torpedo* species have provided estimates of slow and fast desensitization rates. Slow desensitization, which can be monitored in *Torpedo* AChR with manual ion flux assays (Walker et al., 1981; Walker et al., 1982) or binding experiments (Boyd and Cohen, 1980*a*; Neubig et al., 1982), has a maximum rate in the presence of ACh or carbamylcholine (CCh), of ~0.1 $s^{-1}$ (Boyd and Cohen, 1980*a*; Walker et al., 1981; Hess et al., 1982). Maximum rates for fast desensitization determined from rapid quenched-flow ion flux measurements range

[1] *Abbreviations used in this paper:* ACh, acetylcholine; AChR, acetylcholine receptor; $\alpha$-BTX, alpha-bungarotoxin; CCh, carbamylcholine; Dns-$C_6$-Chol, dansyl-$C_6$-choline [1-(5-dimethylamino naphthalene) sulphonamido] *n*-hexanoic acid *b*-(*N*-trimethylammonium bromide) ethyl ester); SubCh, suberyldicholine.

Address correspondence to Keith W. Miller, Department of Anesthesia, Massachusetts General Hospital, Boston, MA 02114.

from 1.5 $s^{-1}$ in native *Torpedo* vesicles (Hess et al., 1982; Takeyasu et al., 1986) to 5.3 $s^{-1}$ in reconstituted vesicles (Walker et al., 1982).

In this paper, we present studies on the kinetics of the third way in which ACh can inactivate channel function: self inhibition. To resolve this phase of inhibition we found it advantageous to pay strict attention to two factors.

First, desensitization rates derived from studies using native *Torpedo* AChR-rich vesicles may be affected by their small internal volumes and high surface AChR densities (Neubig and Cohen, 1980; Forman et al., 1987). If there are more AChR molecules than are required to complete $^{86}Rb^+$ exchange before it can be experimentally terminated, the vesicles can be said to possess "spare receptors" (Furchgott and Bursztyn, 1967). A theoretical analysis of quenched-flow inactivation studies shows that in the presence of spare receptors, the initial rate of decrease of the integrated flux response would be lower than the true inactivation rate (see Appendix).

Second, the time resolution of quenched-flow studies was improved to $^{86}Rb^+$ flux periods of 3 ms and agonist preincubation periods of 8 ms. ACh-induced inactivation kinetics were then investigated in both channel activating and self-inhibiting ranges. ACh, rather than CCh, was chosen for this study because it is the natural ligand for AChR and because concentration-response studies have shown that ACh-induced activation and self inhibition occur in widely separated concentration ranges (Forman et al., 1987).

## MATERIALS AND METHODS

### *Torpedo* Vesicle Preparation

Purification of AChR from freshly killed *Torpedo nobiliana* (Biofish Associates, Georgetown, MA) and determinations of concentration and purity we performed as described previously (Forman et al., 1987). Aliquots of receptor-rich membrane were suspended in *Torpedo* physiological saline (TPS; 250 mM NaCl, 5 mM KCl, 2 mM $MgCl_2$, 3 mM $CaCl_2$, 5 mM $PO_4^{2-}$, 0.02% $NaN_3$; pH 7.0), frozen in liquid nitrogen, and thawed up to 48 h before use. Vesicles were incubated for 20 min with 0.1 mM diisopropylfluorophosphate (DFP) to inhibit acetylcholinesterase activity before flux assays.

### Alpha-Bungarotoxin

$\alpha$-BTX was repurified by ion exchange chromatography on CM-52 cellulose (Whatman, Maidstone, Kent, UK). Partial blockade of AChR function in vesicle membranes was achieved by overnight incubation at 4°C with desired stoichiometric amounts of $\alpha$-BTX. For most quenched-flow studies, 50–60% of [$^3$H]-ACh sites were blocked.

### Rapid Mixing Apparatus

Our apparatus is similar to that described by Cash and Hess (1981), incorporating pneumatically driven syringes connected to both solution reservoirs and a flexible flow system through three-way valves. Ball-type mixing chambers (Berger et al., 1968) were supplied by Research Instruments & Manufacturing Co., San Diego, CA. Actuation of pneumatic drives was controlled by a microcomputer (Apple II+, Cupertino, CA) through a custom-built interface. Pneumatic drive movements (coupled to a sliding variable resistor) were monitored by the computer through a 12-bit analog-to-digital converter.

### Estimation of Initial Flux Rates

All flux studies were performed at 4°C. $^{86}Rb^+$ efflux from native *Torpedo* vesicles was measured with a rapid (3–4 ms) quenched-flow assay and the percentage of nonleak counts ($F_A$) calculated.

$$F_A = \frac{\text{CPM(Ag)} - \text{CPM(leak)}}{\text{CPM(total)} - \text{CPM(leak)}} \times 100. \qquad (1a)$$

Determination of CPM(leak) and CPM(total) have been previously described (Forman et al., 1987). Estimated initial $^{86}Rb^+$ efflux rates ($k_f$) from single time-point data were calculated as first order approximations.

$$k_f = \frac{-ln\,[1 - (F_A\,T/F_{eq})]}{T}, \qquad (1b)$$

where $T$ is the $^{86}Rb^+$ efflux period, determined as described below, and $F_{eq}$ is the measured flux after a long exposure to the maximum activating ACh concentration (usually 10 s with 1 mM ACh).

### Determination of Inactivation Rates

Flow systems for assaying $^{86}Rb^+$ influx after either short or long inactivations in the presence of ACh are shown in Fig. 1. For inactivation times ($t$) between 8 and 30 ms, a continuous double-mix quenched-flow system was used (Fig. 1 *A*). 1 vol of vesicles (syringe V) was sequentially mixed with (at *M1*) 1 vol of desensitizing ACh solution (syringe A), (at *M2*) 1 vol of flux solution containing ACh and 100 $\mu$Ci/ml $^{86}Rb^+$ (syringe $M^+$); and (at *M3*) 1 vol of 200 mM procaine (syringe Q). Variable

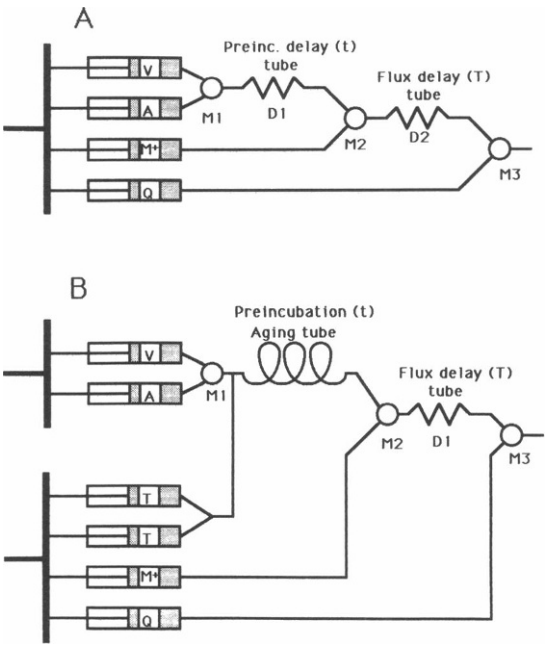


FIGURE 1 Schematic of quenched-flow experimental configurations. (*A*) Double-mix quenched-flow experiment. Syringe V contains AChR-rich vesicles; syringe A contains 2 × desensitizing ACh concentration ($a$); syringe $M^+$ contains both ACh and $^{86}Rb^+$; and syringe Q contains 200 mM procaine "quench." (*B*) Pulsed quenched-flow experiment. Syringes are labeled as above, except syringes T, which contain TPS.

preincubation times ($t$) and influx periods ($T$) were achieved by altering the lengths of D1 and D2, respectively. Passage times through delay tubes were calculated from linear least squares fitted slopes of drive tracings, the known total volume slowing through each section of tubing and the known delay tube volumes. Calculated passage times were within 2 ms of calibration times estimated from base hydrolysis of o-NPA in the apparatus (Neubig and Cohen, 1980).

For inactivation times >70 ms, pulsed quenched-flow (Fig. 1 *B*) was performed essentially as described by Aoshima et al. (1981). Actuation of the first pneumatic ram drove vesicles (syringe V) and desensitizing solution (syringe A) through mixer M1 into an aging tube. After an inactivation delay ($t$), a second pneumatic ram flushed TPS (syringes T) into the aging tube, displacing the vesicle/agonist solution, which was rapidly mixed at M2 with flux solution ($^{86}Rb^+$ and ACh; syringe $M^+$) and then, at M3 with 200 mM procaine (syringe Q). The rates of movement of the two pneumatic rams were carefully matched by adjusting the driving pressures so that all vesicles resided in the aging tube for the same amount of time. Influx time ($T$) was varied by changing the length of D1.

A portion of the quenched vesicle solution was collected by using a sample-and-flush valve with a 175 μl sample loop attached to the outflow of M3. The sample-loop contents were flushed onto a small cation exchange column (Dowex-50Wx8, 100–200 mesh, 1 ml bed volume) with 220 mM sucrose. Vesicles and entrapped $^{86}Rb^+$ were eluted with another aliquot of sucrose solution, mixed with scintillation cocktail, and counted. Passive $^{86}Rb^+$ leak into vesicles was measured either in the absence of agonist or in the presence of 50 mM procaine. Leak corrected $F_A$ values were calculated with Eq. 1a.

Nicotinic AChR channel activity in inactivation studies was determined from the amount of $^{86}Rb^+$ which entered sealed vesicles and expressed as $F^{a,t}_{A,T}$ (see Table I). Superscript variables represent ACh concentration ($a$) and time ($t$) during desensitization, whereas subscript variables represent conditions during $^{86}Rb^+$ flux measurement. When the desensitizing ACh was in the channel activating range (i.e., <1 mM), AChR activity was measured with a 1 mM ACh influx assay. When ACh concentrations above 1 mM (i.e., self-inhibiting range) were used for desensitization, the receptor activity was measured in the presence of the desensitizing ACh concentration. AChR activity before inactivation ($F^{0,0}_{A,T}$) was measured by the same technique used to measure the response after inactivation, except that no ACh was used before $^{86}Rb^+$ exposure (i.e., syringe A contained TPS).

Flux responses were normalized to a maximum control response, $F^{0,0}_{1mM,T}$ determined with each series of experiments. Normalized data from experiments in different time ranges could be combined for analysis. We first analyzed the data assuming a single exponential inactivation described by

$$F^{a,t}_{A,T} = F^{0,0}_{A,T} \times \exp(-k_d \times t), \quad (2)$$

where $k_d$ is the desensitization rate. We plotted $ln[F^{a,t}_{A,T}/F^{0,0}_{1mm,T}]$ vs. inactivation time ($t$) and calculated a linear least squares line using points with $t > 0$. The slope of the fitted line was taken as $k_d$.

TABLE I
DEFINITIONS OF VARIABLES

| Variable | Definition |
|---|---|
| $F_A$ | Integrated flux response in presence of ACh concentration $A$. |
| $F_{eq}$ | Flux response corresponding to full equilibration of $^{86}Rb^+$ across AChR-containing vesicle membranes. |
| $F^{0,0}_{A,T}$ | Integrated flux response (time = $T$) without preincubation (same as $F_A$). |
| $F^{a,t}_{A,T}$ | Integrated flux response after preincubation period $t$ in the presence of ACh concentration $a$. |
| $k_f$ | $^{86}Rb^+$ flux rate constant. |
| $k_d$ | Fast desensitization rate constant. |
| $k_r$ | Rapid inactivation rate constant. |
| $K_A$ | ACh concentration eliciting $F_A$(max)/2 response. |
| $K_B$ | ACh concentration causing 50% self inhibition. |
| $K_D$ | ACh concentration causing desensitization rate $k_d$(max)/2. |

## Chemicals

Diisopropylfluorophosphate (DFP) was from Aldrich Chemical Co., Milwaukee, WI. Alpha-bungarotoxin was from Miami Serpentarium, Miami, FL. Acetylcholine chloride, procaine hydrochloride, and buffer reagents were from Sigma Chemical Co., St. Louis, MO. Radiochemicals: [$^3$H]-ACh was from New England Nuclear, Boston, MA, or Amersham Corp., Arlington Heights, IL. Specific activities were determined by isotope dilution assays (Neubig and Cohen, 1979). $^{86}$RbCl was from New England Nuclear.

## RESULTS

Model analysis of quenched-flow data (Appendix) shows that experimental conditions for accurate determination of inactivation kinetics are achieved when a small fraction of $^{86}Rb^+$ exchange (<0.35 × $F_{eq}$) is allowed when measuring $F^{0,0}_{A,T}$. Two experimental parameters can be modified to establish these conditions: the $^{86}Rb^+$ flux period ($T$) and the rate of $^{86}Rb^+$ exchange across vesicle membranes ($k_f$). Using maximum activating ACh conditions (1 mM ACh), unmodified *Torpedo* AChR vesicles exchanged 0.72 × $F_{eq}$ ($F_{eq}$ represents maximum $^{86}Rb^+$ exchange) in 5 ms. As predicted by the model, the apparent desensitization rate ($k_d$) determined from plots of $ln[F^{a,t}_{A,T}]$ vs. inactivation time ($t$) varies, depending on the points used for linear least squares analysis. When 50% of the ACh channel activation sites on these vesicles are blocked with α-BTX, the 5-ms flux response drops to 0.31 × $F_{eq}$ and $k_d$ is independent of the data points chosen for analysis.

### ACh Concentration-Dependence of $k_d$

Concentration-response curves in α-BTX treated *Torpedo* vesicles for a variety of nicotinic agonists including ACh, CCh, and suberyldicholine are bell-shaped, displaying both agonist-dependent channel activation and self-inhibition at high agonist concentrations (Forman et al., 1987). The concentration-response curves are well described by a biphasic logistic function:

$$F_A = F_A(\max) \times \left(\frac{[A]^{N_1}}{[A]^{N_1} + K_A^{N_1}}\right) \times \left(1 - \frac{[A]^{N_2}}{[A]^{N_2} + K_B^{N_2}}\right), \quad (3)$$

where $F_A$ is the $^{86}Rb^+$ flux response, $K_A$ is the 50% activating agonist concentration, $N_1$ is the Hill coefficient for activation, $K_B$ is the concentration causing 50% self inhibition, and $N_2$ is the Hill coefficient for self inhibition. For ACh, significant channel activation is observed at concentrations above 10 μM, increasing to a maximum response plateau between 1 and 10 mM. Self inhibition is observed above 10 mM ACh.

The time-courses of inactivation with ACh concentra-

tions in both the activating and self-inhibiting ranges were first studied with the pulsed quenched-flow technique (Fig. 2). In particular, we investigated whether inactivation was strictly monoexponential. This was tested by comparing the measured ln $[F^{0,0}_{A,T}]$ with the $y$-axis intercept ($t = 0$) from linear least squares regression of data for $t > 0$. If these two values were the same within one standard error, we considered inactivation to be monoexponential in the time range studied.

With no ACh present during the inactivation pulse, no time-dependent loss of flux activity is observed. Preincubation at the lowest ACh concentration tested (10 $\mu$M) for >20 s or at higher ACh concentrations for <10 s reduces $^{86}Rb^+$ influx into vesicles to the passive leak level ($F^{a,t}_{A,T} = 0$). When the desensitizing ACh is <1 mM, the fitted $y$-intercepts are not significantly different from ln $[F^{0,0}_{1mM,T}]$. Desensitization rate constants ($k_d$), determined from slopes of the fitted lines increase from 0.16 $s^{-1}$ at 10 $\mu$M ACh to 6.3 $s^{-1}$ at 1 mM ACh. In inactivation studies using 15, 50, and 100 mM ACh, $y$-intercepts of the fitted lines (see table in legend) are lower than measured $ln\,[F^{0,0}_{A,T}]$'s; $F^{0,0}_{A,T}/F^{0,0}_{1mM,T}$ ratios are 0.95 ± 0.03, 0.82 ± 0.03, and 0.68 ± 0.05, respectively. Slopes of these lines are all close to the slope observed with 1 mM ACh.

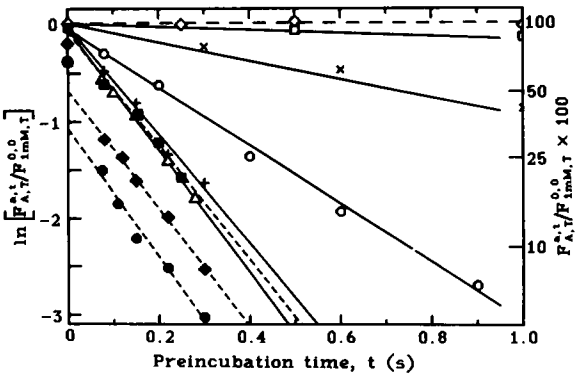


FIGURE 2 Inactivation kinetics under varying ACh desensitization conditions. Vesicles were pretreated with $\alpha$-BTX to block 60% of [$^3$H]-ACh sites. Flux responses ($F^{a,t}_{A,T}$) were measured with a pulsed quenched-flow assay, as described in text and under Methods. Data for inactivation times up to 1 s are shown. Full $t$ range for 0, 10, and 32 $\mu$M ACh are not shown for clarity (two additional points to 20 s, three additional points to 20 s, and three additional points to 4 s, respectively). Calculated flux times ($T$) for most points were from 3.0 to 3.5 ms. In each experimental series, a control flux response with 1 mM ACh ($F^{0,0}_{1mM,T}$) was measured and used to normalize data from different runs. Some flux responses were measured at $T > 3$ ms (up to 13 ms) when activity after inactivation was low. These responses were normalized by measuring at least one point in the experimental set both at 3 ms and at the longer flux time. Data points represent averages of at least three experiments. Plotted lines represent linear least squares fits to data at $t > 0$ (solid for $a \leq 1$ mM Ach and dashed for $a > 1$ mM ACh). Fitted values are as follows:

| Preinc. ACh ($a$) | ln $[F^{0,0}_{A,T}/F^{0,0}_{1mM,T}]$ | $F^{0,0}_{A,T}/F^{0,0}_{1mM,T}$ | $k_d$ |
|---|---|---|---|
| | | | $s^{-1}$ |
| 0 (◇) | 0.03 ± 0.06 | 1.03 ± 0.06 | 0.01 ± 0.03 |
| 10 $\mu$M (□) | −0.04 ± 0.02 | 0.96 ± 0.02 | 0.16 ± 0.02 |
| 32 $\mu$M (×) | 0.05 ± 0.04 | 1.05 ± 0.04 | 0.94 ± 0.08 |
| 100 $\mu$M (○) | −0.06 ± 0.05 | 0.94 ± 0.05 | 3.2 ± 0.2 |
| 320 $\mu$M (+) | −0.02 ± 0.04 | 0.98 ± 0.04 | 5.6 ± 0.2 |
| 1 mM (△) | −0.05 ± 0.05 | 0.95 ± 0.05 | 6.3 ± 0.3 |
| 15 mM (■) | −0.08 ± 0.04 | 0.92 ± 0.04 | 5.9 ± 0.4 |
| 50 mM (▲) | −0.69 ± 0.08 | 0.50 ± 0.04 | 6.1 ± 0.2 |
| 100 mM (●) | −1.09 ± 0.23 | 0.34 ± 0.08 | 6.6 ± 0.5 |

Apparent $k_d$s for all ACh concentrations were also derived from nonlinear least squares fits of flux data to Eq. 2 and are close to the slopes of the fitted lines in Fig. 2. Fitted $k_d$s are plotted against ACh concentration in Fig. 3 (*open squares*). They show a sigmoidal dependence on ACh and were fitted to the following logistic function by nonlinear least squares.

$$k_d = k_d\,(\max) \times \left(\frac{[A]^{N_D}}{[A]^{N_D} + K_D^{N_D}}\right). \quad (4)$$

$K_D$ is the ACh concentration causing a desensitization rate of $k_d$(max)/2 and $N_D$ is the Hill coefficient for ACh-dependent desensitization. The data in Fig. 3 are fitted by $k_d$(max) = 6.6 ± 0.2 $s^{-1}$, $K_D$ = 102 ± 16 $\mu$M, and $N_D$ = 1.6 ± 0.3. Two other receptor preparations (not shown) were characterized by $k_d$(max) values of 8.0 ± 0.3 $s^{-1}$ and 6.9 ± 0.5 $s^{-1}$.

For comparison to the $k_d$ vs. ACh curve, we also plotted initial $^{86}Rb^+$ efflux rates ($k_f$s estimated using Eq. 1b), vs. ACh over the activating ACh range (Fig. 3, *solid circles*). The $k_f$ vs. ACh curve closely parallels the $k_d$ vs. ACh curve. Nonlinear least squares fitting to a logistic function (Eq. 3, with $k_f$ instead of $F_A$ and $K_B = \infty$), gives $k_f$(max) = 94 ± 8 $s^{-1}$, $K_A$ = 77 ± 18 $\mu$M, and $N_1$ = 1.7 ± 0.2.

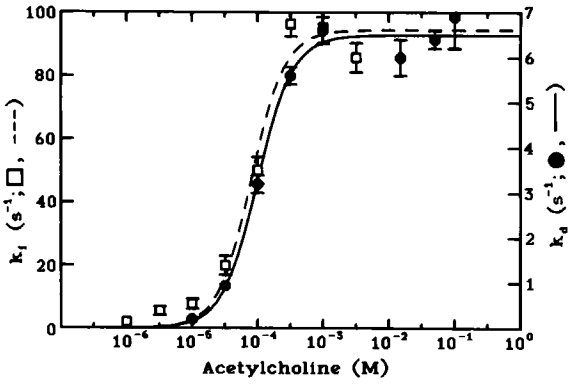


FIGURE 3 ACh concentration-response curves for flux rate and desensitization rate. Initial efflux rates ($k_f$s from Eq. 1b in text; ○) were estimated from averaged ($N \geq 3$; vertical bars indicate 1 SD) flux measurements in a single batch of $\alpha$-BTX–treated vesicles (60% block). The dashed line represents a nonlinear least squares fit to data using Eq. 3 with $k_f$ substituted for $F_A$ and $K_B = \infty$. Fitted parameters are $k_f$(max) = 94 ± 8 $s^{-1}$, $K_A$ = 77 ± 18 $\mu$M, and $N_1$ = 1.7 ± 0.2. Desensitization rates ($k_d$s; solid ●) were calculated from data in Fig. 2 using nonlinear least squares fits to Eq. 2. The solid line represents a nonlinear least squares fit to data using Eq. 4 in text. Fitted values are; $k_d$(max) = 6.6 ± 0.2 $s^{-1}$, $K_D$ = 102 ± 16 $\mu$M, and $N_D$ = 1.6 ± 0.3.

## Rapid Inactivation at High ACh

Pulsed quenched-flow results show that extrapolated $y$-intercepts are lower than measured ln $[F^{0,0}_{A,T}]$ values with 15, 50, and 100 mM ACh (Fig. 2), indicating the presence of an early (within 75 ms) inactivation of AChR. This rapid inactivation phase at 50 and 100 mM ACh ("rapid" indicating faster than "fast" desensitization) was further investigated with a continuous double-mix quenched-flow assay, which enabled measurements of inactivation effects between 8 and 30 ms (Fig. 4 *B*). For a control, we also performed double-mix quenched-flow studies using 1 mM ACh. With 1 mM ACh, 15% inactivation is observed after a 24-ms preincubation, indicating an inactivation rate of 6.8 $s^{-1}$. At 50 mM ACh, flux dropped from 80% of control ($F^{0,0}_{1mM,T}$) at $t = 0$ to 38% of control in 30 ms, whereas 100 mM ACh caused a drop from 68% to 25% of control in under 25 ms. To obtain estimates of rapid inactivation rates, normalized data from both double-mix and pulsed experiments were combined (Fig. 4 *A*) and fitted to a double exponential function.

$$F^{a,t}_{A,T}/F^{0,0}_{1mM,T} = I_r \times \exp(-k_r \times t) + I_d \times \exp(-k_d \times t), \quad (5)$$

where $I_r$ and $I_d$ are the fractions of rapid inactivation and fast desensitization, respectively, and $k_r$ and $k_d$ are the exponential rate constants. Rapid inactivation rates from fits to Eq. 5 ($k_r = 85 \pm 18$ $s^{-1}$ and $155 \pm 27$ $s^{-1}$ at 50 and 100 mM ACh) are 10- to 20-fold higher than $k_d$s from Fig. 2, while the $k_d$s derived from biphasic analysis are near the earlier values. $I_r$ values for both biphasic curves are about the same, but because $F^{0,0}_{A,T}$ is lower at 100 mM ACh than at 50 mM, the extent of rapid inactivation is relatively higher at 100 mM ACh. Fig. 4 *B* shows the first 40 ms of the fitted inactivation curves, illustrating that back-extrapolations of the rapid phases reach the control flux level at $t = -4.5$ ms with 50 mM, and at $t = -3.7$ ms with 100 mM ACh.

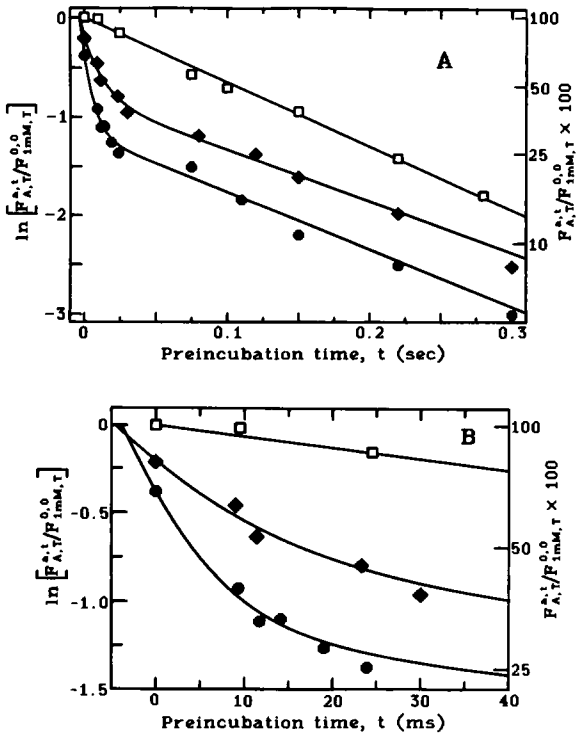


FIGURE 4 Rapid inactivation at 50 and 100 mM ACh. (*A*) Vesicles were pretreated with $\alpha$-BTX to block 60% of [$^3$H]-ACh sites. Flux responses ($F^{a,t}_{AT}$) after preincubation periods < 30 ms were measured by double-mix quenched-flow and combined with normalized data points from Fig. 2. Calculated flux times ($T$) were between 3.0 and 3.3 ms. Data was normalized to $F^{0,0}_{1mM,T}$, as described for Fig. 2. Data points represent averages of at least three experiments. Line through 1 mM ACh data represents a linear least squares fit. Curves through 50 and 100 mM ACh data points represent nonlinear least squares fits to Eq. 5. Fitted parameters are: 1 mM ACh (□): intercept = $0.02 \pm 0.05$ ($1.02 \times F^{0,0}_{1mM,T}$), slope = $-6.5 \times 0.2$ $s^{-1}$. 50 mM ACh (♦): $I_r = 0.37 \pm 0.04$, $k_r = 84.5 \pm 18$ $s^{-1}$, $I_d = 0.44 \pm 0.04$, $k_d = 5.3 \pm 0.7$ $s^{-1}$. 100 mM ACh (●): $I_r = 0.38 \pm 0.03$, $k_r = 155 \pm 27$ $s^{-1}$, $I_d = 0.30 \pm 0.02$, $k_d = 5.9 \pm 0.8$ $s^{-1}$. (*B*) The first 40 ms of Fig. 4 *A* is shown on a larger scale.

# DISCUSSION

## Effects of Spare Receptors

By combining the use of very short tracer flux assay periods with $\alpha$-BTX-treated *Torpedo* vesicles, we eliminated a number of problems encountered when studying inactivation kinetics in native *Torpedo* vesicles. In the experiment described in the Appendix to this paper (Fig. 5), the initial $^{86}Rb^+$ flux rate ($k_f$) before $\alpha$-BTX treatment was too high to accurately measure with a 5 ms flux assay. The inactivation rate ($k_d$) determined from the resulting nonlinear ln ($F_A$) vs. $t$ plot depends on the set of points chosen for linear analysis (2.9 $s^{-1}$ initially, increasing to 4.9 $s^{-1}$ after 75 ms). After irreversible blockade of half of the ACh sites, the flux rate decreases, the plotted data are linear, and the apparent $k_d$ increases (6.7 $s^{-1}$).

Spare receptors in *Torpedo* vesicles have previously been cited as a problem in determination of inactivation rates (Hess et al., 1982; Heidmann et al., 1983). The strategy adopted by Hess et al. (1982) was to use the agonist-induced inactivation process to reduce $^{86}Rb^+$ flux rates to "measurable" levels. At their most potent agonist concentration (10 mM CCh), inactivation for at least 200 ms was required before flux levels decreased in a time-dependent manner. Initial flux rates were estimated by back extrapolation (inactivation was assumed to be mono-exponential). Heidmann et al. (1983) attempted to overcome the spare receptor problem by using the fluorescent agonist, Dns-$C_6$-Chol, which elicits much lower initial flux rates than ACh. The low flux is probably caused, as with other partial agonists (Adams and Sakmann, 1978), by Dns-$C_6$-Chol self-inhibition occurring in the same concentration range as activation (i.e., $K_B \simeq K_A$ in Eq. 3; Forman et al., 1987). The analytical method used by Heidmann et al. fitted flux data to a function in which both $k_f$ and $k_d$ were variables, providing accurately fitted $k_d$s only when they were comparable to $k_f$.

In the present study, measured responses ($F_A$s) were proportional to $^{86}Rb^+$ flux rates, enabling us to directly measure the pre-desensitized response ($F^{0,0}_{A,T}$) and effects of very short inactivation periods. Using $\alpha$-BTX to reduce $k_f$ has been criticized (Hess et al., 1982) because toxin binding may affect the interaction of agonists with AChR. However, Sine and Taylor (1980) showed that $\alpha$-BTX, which binds without preference to two ACh sites on the AChR monomer, prevents agonist-mediated channel opening in BC3H1 cells when bound to either one or both sites. Thus, flux signal is contributed only by unmodified AChRs, which are present at a relative concentration of $(1 - X)^2$, where $X$ is the fraction of toxin-bound ACh sites. Concentration-response curves for AChR activation by CCh both without (Walker et al., 1981) and with (Neubig and Cohen, 1980; Forman et al., 1987) partial $\alpha$-BTX blockade are similar. In the experiment described in our Appendix, the estimated $k_f$ was reduced by ~70% after 50% $\alpha$-BTX blockade, consistent with Sine and Taylor's conclusions.

## ACh Concentration-Dependence of $k_d$

Over the entire range of desensitizing ACh concentrations studied (10 $\mu$M to 100 mM), $ln\ [F^{a,t}_{A,T}]$ vs. $t$ data at 75 ms < $t$ were well fitted by straight lines (Fig. 2). In addition, $y$-intercepts of fitted lines with ACh between 10 $\mu$M and 1 mM, differed by <5% from measured ln $[F^{0,0}_{A,T}]$ values. We conclude that desensitization in the presence of <1 mM ACh is monophasic at times <1 s. Others have shown that a slow phase of desensitization (0.1 $s^{-1}$ and below) is observable in *Torpedo* vesicles (Walker et al., 1981; Hess et al., 1982; Walker et al., 1982) and at the amphibian neuromuscular junction (Sakmann et al., 1980; Feltz and Trautmann, 1982; Chestnut, 1983) after fast desensitization. This slow phase was not observed in our study, because fast desensitization with >10 $\mu$M ACh eliminated essentially all cation channel activity. However, our results do not exclude the presence of slow desensitization, because the flux times ($T$) used were not long enough to enable detection of very low flux rates remaining after rapid desensitization.

Results summarized in Fig. 3 show that the ACh concentrations at the half-maximal fast desensitization rate ($K_D$ in Eq. 4) and the half-maximal $^{86}Rb^+$ flux rate ($K_A$) are not significantly different and that the Hill coefficients for desensitization and flux are close ($N_D$ = 1.6 compared with $N_l$ = 1.7). This strongly suggests that both fast desensitization and cation channel opening are triggered by ACh binding to two activation sites. In Figs. 2 and 3, $k_d$s estimated from pulsed quenched-flow data at 15, 50, and 100 mM ACh are close to the $k_d$ at 1 mM ACh. This plateau in $k_d$ at agonist concentrations above those that saturate ACh activation sites was previously observed at up to 10 mM ACh in *Torpedo* (Takeyasu et al., 1986; Huganir et al., 1986) and with both ACh and suberyldicholine in *Electrophorus* vesicles (Pasquale et al., 1983; Takeyasu et al., 1983).

Maximum $k_d$s in this study are three- to fourfold higher than those from previous reports of quenched-flow experiments in native *Torpedo* vesicles at 0–4°C (Walker et al., 1981; Hess et al., 1982; Takeyasu et al., 1986). Although most previous measurements were made in *Torpedo californica,* which may display different inactivation kinetics, the lower $k_d$s derived in other studies might be attributed to the presence of spare receptors. Indeed, our $k_d$(max) values are comparable to rates derived from experiments using *Torpedo californica* receptor reconstituted into vesicles (5.3 $s^{-1}$; Walker et al., 1982) and *Electrophorus* vesicles (7 $s^{-1}$; Cash et al., 1981; Hess et al., 1982). Like $\alpha$-BTX blocked vesicles, these systems are also characterized by low $^{86}Rb^+$ flux rates.

## Mechanism of Fast Desensitization

Katz and Thesleff (1957) originally proposed that desensitization is triggered by agonist binding to channel activation sites, but the nature of the ACh-bound state(s) from which desensitization proceeds has remained uncertain. Slow desensitization is known to proceed at ACh concentrations where negligible channel opening occurs and the Hill coefficient for slow rates is 1.0 (Neubig et al., 1982). Consequently, it has been suggested that slow desensitization occurs from a singly-liganded AChR state (i.e., only one activating site bound to agonist). Consistent with this scheme, an irreversibly bound agonist analogue, bromoacetylcholine, also blocks agonist binding to desensitized receptors (Damle and Karlin, 1978; Wolosin et al., 1980).

Previous quenched-flow results in both *Electrophorus* (Aoshima et al., 1981; Cash and Hess, 1981) and *Torpedo* vesicles (Hess et al., 1982; Heidmann et al., 1983; Takeyasu et al., 1986; Huganir et al., 1986) are consistent with a model where fast desensitization occurs from a doubly-liganded "pre-open" AChR state in rapid equilibrium with the open channel state (Hess et al., 1983). Results that argue against this model are rather conflicting. In reconstituted AChR, Walker et al. (1982) found $K_D > K_A$ and $N_D$ close to 1.0, while ligand binding studies using [$^3$H]-ACh (Boyd and Cohen, 1980*b*) indicate $K_D < K_A$. Our results support a mechanism where fast desensitization occurs from all doubly-liganded AChR states (to be discussed further).

## Rapid Inactivation

With 50 and 100 mM ACh, pulsed quenched-flow experiments revealed an AChR inactivation process occurring before fast desensitization, which we have termed rapid inactivation. A continuous double-mix quenched-flow experiment resolved the time-course of rapid inactivation. ACh-induced inactivation on this time scale has been previously reported in studies of frequency-dependent

nerve stimulation at the frog neuromuscular junction (Magleby and Pallotta, 1981).

Rapid inactivation is almost certainly the same process as the self inhibition by agonists observed in integrated flux experiments. Both the rate and extent of rapid inactivation increase in parallel with self inhibition observed in integrated flux assays (Forman et al., 1987). Rapid inactivation cannot be the result of higher rates of fast desensitization at very high ACh, as suggested by Walker et al. (1982), because rapid inactivation rates ($k_r$) are 10- to 20-fold higher than $k_d$(max), which shows a clear plateau between 1 and 15 mM ACh. Additional inactivation phases with rates matching $k_d$(max) are observed after rapid inactivation is complete with both 50 and 100 mM ACh.

Back-extrapolations of the rapid inactivation phases in curves from Fig. 4 *B* intersect the $F^{0,0}_{1mM}$ value at about $t = -4$ ms, close to the flux assay times calculated from tracings of pneumatic ram movements plus mixing times for ball-type cells used in our apparatus (estimated at ~0.3 ms; Berger et al., 1968). Thus, the $F^{0,0}_{A,T}$ values observed with 50 and 100 mM ACh may be attributed to rapid inactivation during the flux assay. To test this possibility, we calculated integrated flux reponses in the presence of both rapid inactivation and fast desensitization with the following equation, analogous to the equation derived by Neubig and Cohen (1980) for desensitization alone.

$$F_{A,T} = F_{eq} \times \left[1 - \exp\left(-k_f\left\{\frac{I_r}{k_r}[1 - \exp(-k_r T)] + \frac{I_d}{k_d}[1 - \exp(-k_d T)]\right\}\right)\right], \quad (6)$$

where parameters are defined as in Eq. 5 (also see Table I) and $I_r + I_d = 1$. For calculations of integrated flux in the presence of 1, 50, and 100 mM ACh, $k_f$ was set at the experimental $k_f$(max) (94 $s^{-1}$). Other parameters were set at the values derived from analysis of Fig. 4 *B*, except $I_r$, which was set at $1 - I_d$.

For a flux time ($T$) of 3.5 ms, Eq. 6 predicts $F_{50mM}/F_{1mM} = 0.93$ (7% inhibition) and $F_{100mM}/F_{1mM} = 0.85$ (15% inhibition). Measured $F^{0,0}_{A,3.5ms}$ values in Fig. 4 show significantly more self inhibition than these calculations, indicating that some portion of the self-inhibition process may be occurring at rates beyond the time resolution of our rapid-mixing apparatus. Simulations with Eq. 6 predict observed $F^{0,0}_{A,3.5ms}$ values for 50 and 100 mM ACh when $k_r$s are 340 $s^{-1}$ and 480 $s^{-1}$, respectively.

## Mechanisms of Self Inhibition

Both allosteric and channel blocking mechanisms for self inhibition have been proposed (see Pasquale et al., 1983). Both mechanisms assume a bimolecular interaction between ACh and a self-inhibition site:

$$B + \mathcal{R} \underset{k_{off}}{\overset{k_{on}}{\rightleftharpoons}} \mathcal{R}B \quad (7a)$$

In this model, B represents the inhibitory ligand (ACh), and $\mathcal{R}$ represents those receptor states possessing a self-inhibition site (e.g., unbound receptor, receptor with one ACh activating site occupied, receptor with both activating sites occupied, receptors with open cation channels, and desensitized receptor). The observed rate of rapid inactivation is

$$k_r = k_{off} + (B \times k_{on}). \quad (7b)$$

Although it is not known which AChR states are inhibited, self-inhibiting ACh concentrations are much higher than the dissociation constant for activation sites ($K_A$ in Eq. 3), so that the distribution of AChR states before binding the inhibitory site is invariant with ACh concentration (note that when $K_B$ is close to $K_A$, as with partial agonists, this is not the case; Forman et al., 1987). The dissociation constant for binding to the self-inhibition site is:

$$K_B = [B] \times \frac{[\mathcal{R}]}{[\mathcal{R}B]} = \frac{k_{off}}{k_{on}}. \quad (7c)$$

Because rapid inactivation is essentially complete (i.e., at equilibrium) before fast desensitization, the ratio of noninhibited to inhibited receptors in scheme 7a can be estimated from analysis of biphasic inactivation curves as $[\mathcal{R}]/[\mathcal{R}B] = I_d/I_r$. Using $I_d$ values from analysis of Fig. 4 and setting $I_r = 1 - I_d$, in Eq. 7c, we derive $k_{on} = 950$ $M^{-1}s^{-1}$ and $k_{off} = 37$ $s^{-1}$ ($K_B = 39$ mM) for data at 50 mM ACh, and $k_{on} = 1{,}080$ $M^{-1}s^{-1}$ and $k_{off} = 47$ $s^{-1}$ ($K_B = 43$ mM) at 100 mM ACh, two independent estimates that do not differ significantly from each other. $K_B$s derived from this analysis are in excellent agreement with values for ACh self inhibition reported from both single channel studies in BC3H1 cells (50 mM; Sine and Steinbach, 1984) and flux studies in *Electrophorus* vesicles (50 mM; Takeyasu et al., 1986).

Our results show that self inhibition may occur only after channel activation, suggesting a mechanism in which agonists bind selectively to open channels. This mechanism predicts that initial $^{86}Rb^+$ flux rates are not reduced unless channel inhibition occurs much faster than $^{86}Rb^+$ flux. Our data also require that the blocked state may directly desensitize without reopening, since a sequential block model where only unblocked channels desensitize predicts incorrectly that the rate of desensitization will decrease at self-inhibiting ACh concentrations. A mechanism in which all multiply-liganded receptor states (including the open channel and blocked states) desensitize at the same rate (Pasquale et al., 1983) is most compatible with available data. Desensitization from the inhibitor-bound state is also supported by evidence that inhibitors reduce integrated

flux over long times (Neher, 1983), as observed with both suberyldicholine and (−)-nicotine in *Torpedo* vesicles using 10 s $^{86}Rb^+$ flux (Forman et al., 1987). In addition, channel blockers remain "trapped" within AChR channels after ACh dissociates (Gurney and Rang, 1984; Neely and Lingle, 1986).

Support for selective binding to open channels comes from single-channel traces in the presence of self-inhibiting agonist doses (Sine and Steinbach, 1984; Ogden and Colquhoun, 1985), which show rapid closing events within channel openings, similar to those seen with local anesthetics (Neher and Steinbach, 1978). The self-inhibitory potencies of agonists are voltage dependent (Sine and Steinbach, 1984; Takeyasu et al., 1986; Ogden and Colquhoun, 1985), as are the potencies of local anesthetics, indicating a site partway across the membrane voltage gradient (Adams, 1977). Recent studies in *Torpedo* (Heidmann and Changeux, 1986) also show that [$^3$H]-chlorpromazine, a noncompetitive inhibitor, selectively photolabels open channels, but does not bind to either resting or desensitized AChR. Our low $k_{on}$ could be attributed to a diffusion barrier in this model. One possibility is that the blocking site is on the cytoplasmic side of the membrane. Indeed, there is evidence that agonists pass through the AChR channel (Case et al., 1977; Sine and Steinbach, 1984) and that the site of local anesthetic inhibition on AChR may be intracellular (Gage et al., 1983).

An alternative mechanism where agonists bind to an allosteric self-inhibitory site accessible on all receptor states with equal affinity has been proposed (Pasquale et al., 1983; Shiono et al., 1984; Takeyasu et al., 1986). The difficulty with this model is that self inhibition occurs simultaneously with activation, reducing initial ion flux rates. Because our $k_{on}$ rates for self-inhibitor binding are four to five orders of magnitude slower than diffusion-limited bimolecular association rates for ACh binding to the activation sites on AChR ($10^6$ to $10^8$ $M^{-1}s^{-1}$; Boyd and Cohen, 1980*b*; Lester and Nerbonne, 1982), the allosteric model must be modified so that either binding of ACh to the allosteric site is slow or a rate limiting conformational change leading to channel inhibition occurs after a diffusion-limited binding step (Neher and Steinbach, 1978).

At present, there is no data that conclusively supports either the allosteric site model or the channel block model for self inhibition by agonists. These two models might be distinguished by determining whether rapid inactivation rates depend linearly (block model with rate-limiting bimolecular association step) or hyperbolically (saturable allosteric site) on ACh concentration. In this study, the range of rapid inactivation rates (and therefore ACh concentrations) was limited by the quenched-flow method. Unfortunately, recently introduced spectrophotometric stopped-flow methods (Karpen et al., 1983) and rapid perfusion electrophysiological techniques (Brett et al., 1986) do not give significantly better time resolution than quenched-flow. A more sensitive test of the two mechanisms may be provided by noncompetitive antagonists, which inhibit AChR function in a manner similar to agonists. A noncompetitive inhibitor that acts at the self-inhibition site for agonists could be used to determine directly whether or not the site is accessible before channel activation.

## APPENDIX

### Model Analysis of Spare Receptor Effects

We initially develop a simple model of our quenched-flow influx experiment for measurement of agonist-induced inactivation rates. As described in Methods, vesicles are first exposed to the desired concentration of ACh ($a$) for a period ($t$) of inactivation. The inactivated vesicle solution is then mixed with a solution containing ACh (at concentration $A$) and $^{86}Rb^+$ for a second short time, $T$, before the flux reaction is quenched with flux-inhibiting drugs. In this analysis, we assume that $^{86}Rb^+$ influx into vesicles follows simple two-compartment kinetics where the internal vesicle volume is negligibly small in comparison with the total reaction volume. In the absence of desensitization, the flux signal, $F_A$ (see Table I for definitions of variables), increases with $T$.

$$F_{A,T} = F_{eq} \times [1 - \exp(-k_f^o \times T)], \quad \text{(A1)}$$

where $k_f^o$ is the initial rate constant for $^{86}Rb^+$ influx into vesicles in the presence of ACh at concentration $A$, and $F_{eq}$ is the $^{86}Rb^+$ content of ACh-activated vesicles after full equilibration across membranes (see Methods). We also assume that the flux rate decreases exponentially during desensitization.

$$k_f^i = k_f^o \times \exp(-k_d \times t), \quad \text{(A2)}$$

where $k_d$ is the true rate of desensitization in the presence of the experimental agonist concentration, $a$. $T$ is short enough so that little or no desensitization occurs during $^{86}Rb^+$ influx. With these conditions, the flux signal is

$$F_{A,T}^{a,t} = F_{eq} \times \{1 - \exp[-k_f^o \times T \times \exp(-k_d \times t)]\}. \quad \text{(A3)}$$

Following the methods used elsewhere in this paper, we plot $ln[F_{A,T}^{a,t}$ (normalized to $F_{eq}$) vs. inactivation time (expressed in units of $k_d^{-1}$).

Fig. 5 *A* illustrates that the shape of the relationship between $F_{A,T}^{a,t}$ and $t$ depends on the dimensionless parameter $k_f^o \times T$, which also determines the response observed before desensitization ($F_{A,T}^{0,0}/F_{eq}$; Eq. A1). At $k_f^o \times T$ values of 0.1 and 0.3 the curves shown in Fig. 5 *A* are approximately linear with the ideal slope of 1.0, indicating the true desensitization rate, while their intercepts on the $y$-axis indicate that flux signal will be only 9.5 and 26% of $F_{eq}$, respectively. At higher $k_f^o \times T$ values, the initial slope of the curves decrease, but approach 1.0 at longer and longer times. For example, with $k_f^o \times T = 5.0$, our model predicts that $F_{A,T}^{0,0}/F_{eq}$ decreases by only 16% after an e-fold decrease in $k_f$ (at $k_d \times t = 1.0$).

### Experimental Effects of Spare Receptors

Fig. 5 *B* shows data from pulsed quenched-flow inactivation experiments using two aliquots from a single batch of AChR vesicles. One aliquot (solid O) was incubated overnight with a 50% stoichiometric amount of $\alpha$-BTX, whereas the other (solid □) was incubated overnight with the same volume of TPS. Inactivation and 5 ms $^{86}Rb^+$ flux were in the presence of 1 mM ACh and flux measurements were normalized to $F_{eq}$s for comparison to Fig. 5 *A*. $F_{eq}$ values (Table I, Methods), measured with 1 mM ACh and 10 s manual influx assays were 80 ± 3% for the unblocked aliquot and 74 ± 5% for the $\alpha$-BTX–treated aliquot.

Blockade with $\alpha$-BTX reduced the preincubation response, $F_{1\,mM,5\,ms}^{0,0}$, by 53% whereas estimated $k_f^o$ (Eq. 1b) was reduced by 71% (from 250 to 73 $s^{-1}$). Given that $k_f^o \times T$ parameters characterizing the blocked and

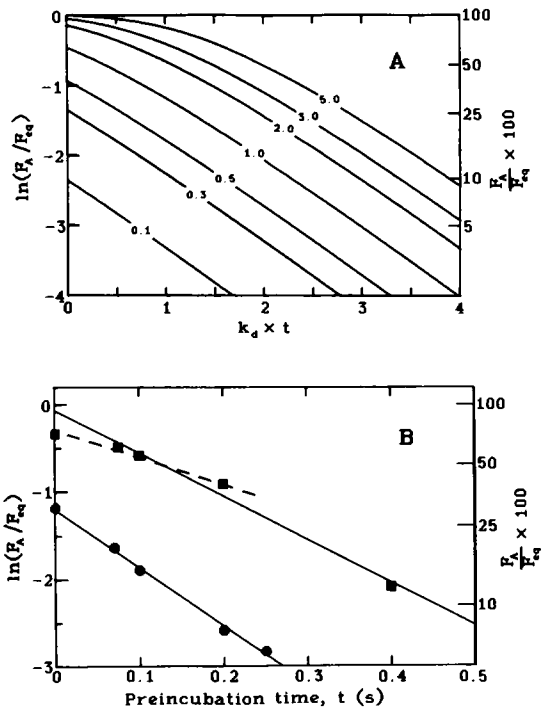


FIGURE 5 Apparent desensitization kinetics under varying flux assay conditions. (*A*) Curves represent desensitization kinetics predicted by Eq. A3. The abscissa is a time axis which has been normalized to the intrinsic desensitization rate, $k_d$, and is therefore dimensionless. Values overlaid on curves are $k_f^o \times T$ conditions for the flux assay, where $k_f^o$ is the initial vesicle flux rate. (*B*) Desensitization kinetics at 1 mM ACh before and after removal of spare receptors. Flux responses after preincubation with ACh (in pulse mode) were measured with a 5-ms quenched-flux assay and normalized to $F_{eq}$, which was measured with a manual 10 s influx assay. Points represent averages of at least three runs. $F_{A,5ms}^{0,0}$ values were measured by preincubating with TPS instead of ACh solution. Solid lines through data represent linear least squares fits to data points with $t > 0$. Untreated vesicles (■); fitted slope = $-4.9 \pm 0.4\ s^{-1}$, fitted intercept = $-0.07 \pm 0.10$, equivalent to $0.93 (\pm 0.09) \times F_{eq}$. $F_{A,5ms}^{0,0} = 0.72 (\pm 0.06) \times F_{eq}$, significantly different from the fitted intercept ($P < 0.05$). The dashed line through untreated vesicle data was calculated for $0 \le t \le 0.2$ s; fitted slope = $-2.9 \pm 0.2\ s^{-1}$, fitted intercept = $0.31 \pm 0.03$, equivalent to $0.73 (\pm 0.02) \times F_{eq}$. Vesicles with 50% [$^3$H]-ACh sites blocked by $\alpha$-BTX (●); fitted slope = $-6.7 \pm 0.4\ s^{-1}$, fitted intercept = $-1.2 \pm 0.1$, equivalent to $0.30 (\pm 0.03) \times F_{eq}$; $F_{A,5ms}^{0,0} = 0.31 (\times 0.03) \times F_{eq}$.

unblocked vesicles are 0.37 and 1.25, respectively, the data in Fig. 5 *B* closely resemble the predictions of the analytical model (Fig. 5 *A*). Linear least squares analysis of $\ln[F_{A,T}^{a,t>0}]$ vs. $t$ data (i.e., omitting the $t = 0$ points) are shown in Fig. 5 *B* (*solid lines*). The fitted line for data from unblocked vesicles has a slope of $-4.9\ s^{-1}$ and $y$-intercept corresponding to $0.93 \times F_{eq}$. This back-extrapolated $t = 0$ response is significantly higher than the measured $F_{1mM,T}^{0,0}$ ($P < 0.05$). The apparent initial rate of fast desensitization for the unblocked vesicles was derived from a linear least squares fit to data points at $t < 0.4$ s (*dashed line*, slope = $2.9\ s^{-1}$). This is 40% lower than the slope of the solid line, illustrating that apparent desensitization rates can vary markedly when $k_f^o \times T$ is high. In contrast, data from 50% blocked vesicles gives a slope of $-6.7\ s^{-1}$ and a $y$-intercept of $0.30 \times F_{eq}$, close to the measured $F_{1mM,T}^{0,0}$.

The above analysis and experimental data clearly show that interpretation of inactivation kinetics is improved when $k_f^o \times T$ is low, because the apparent desensitization rate varies at high $k_f^o \times T$ values. In the present study, our methods were sensitive to changes of $0.03 \times F_{eq}$, and we used $\alpha$-BTX blockade levels that resulted in $F_{A,T}^{0,0}/F_{eq} \le 0.35$ ($k_f^o \times T \le 0.43$). Empirically, we found that $k_d$s determined from a single AChR batch differed by <10%.

Our model also suggests two important caveats when interpreting quenched-flow inactivation data. Firstly, the presence of multiple rapid inactivation processes, such as those described in the present study, may be masked when $k_f^o \times T$ is high, because $F_{A,T}^{a,t}$ at low $t$ values reflect a lower apparent inactivation rate than the true rate. This is reflected in the concave downward curves in Fig. 5 *A*. As demonstrated in our pulsed quenched-flow studies at low $k_f^o \times T$, inactivation processes occurring more rapidly than the shortest experimental inactivation period ($t$), but slower than the flux assay ($T$) were revealed by back-extrapolated $y$-intercepts from $\ln[F_{A,T}^{a,t}]$ vs. $t$ data ($t > 0$) that were lower than the experimental $\ln[F_{A,T}^{0,0}]$. This observation correctly suggested a concave upward inactivation curve.

Secondly, for accurate analysis of agonist-dependent changes in $k_d$, it is best to use standard conditions for flux activity assays. If the test agonist concentration is varied (e.g., when the concentration during $^{86}Rb^+$ influx [$A$] is matched to the desensitizing concentration [$a$]), a systematic underestimation of $k_d$ that increases with agonist concentration may be introduced. This error will cause the apparent slope (Hill coefficient) of $k_d$ vs. agonist plots to be underestimated.

We thank Prof. Richard J. Kitz for his support and Paul Wankowicz for assistance in design and construction of the rapid mixing apparatus.

Supported by National Institute of General Medical Sciences grant GM-15904. S.A.F. was supported by United States Public Health Service Award 2T32GM07753 and by the Department of Anesthesia, Massachusetts General Hospital.

*Received for publication 29 June 1987 and in final form 23 March 1988.*

## REFERENCES

Adams, P. R. 1977. Voltage-jump analysis of procaine action at frog end-plate. *J. Physiol. (Lond.).* 268:291–318.

Adams, P. R., and B. Sakmann. 1978. Decamethonium both opens and blocks endplate channels. *Proc. Natl. Acad. Sci. USA.* 75:2994–2998.

Aoshima, H. D. J. Cash, and G. P. Hess. 1981. Mechanism of inactivation (desensitization) of acetylcholine receptor: investigations by fast reaction techniques with membrane vesicles. *Biochemistry.* 20:3467–3474.

Berger, R. L., B. Balko, and H. F. Chapman. 1968. High resolution mixer for the study of the kinetics of rapid reactions in solution. *Rev. Sci. Instr.* 39:493–498.

Boyd, N. D., and J. B. Cohen. 1980a. Kinetics of binding of [$^3$H]-ACh and [$^3$H]-CCh to *Torpedo* postsynaptic membranes: slow conformational transitions of the cholinergic receptor. *Biochemistry.* 19:5344–5352.

Boyd, N. D., and J. B. Cohen. 1980*b*. Kinetics of [$^3$H]-ACh binding to *Torpedo* postsynaptic membranes: association and dissociation rate constants by rapid mixing and ultrafiltration. *Biochemistry.* 19:5353–5358.

Brett, R. S., J. P. Dilger, P. R. Adams, and B. Lancaster. 1986. A method for the rapid exchange of solutions bathing excised membrane patches. *Biophys. J.* 50:987–992.

Case, R., R. Creese, W. J. Dixon, F. J. Massey, and D. B. Taylor. 1977. Movement of labeled decamethonium in muscle fibres of the rat. *J. Physiol. (Lond.).* 272:283–294.

Cash, D. J., and G. P. Hess. 1981. Quenched flow technique with plasma membrane vesicles: acetylcholine receptor-mediated transmembrane ion flux. *Anal. Biochem.* 112:39–51.

Cash, D. J., H. Aoshima, and G. P. Hess. 1981. Acetylcholine-induced cation translocation across cell membranes and inactivation of the acetylcholine receptor: chemical kinetic measurements in the millisecond time region. *Proc. Natl. Acad. Sci. USA.* 78:3318–3322.

Changeux, J.-P., A. Devillers-Thiery, and P. Chermouilli. 1984. Acetyl-

choline receptor: an allosteric protein. *Science (Wash. DC).* 335:1335–1345.

Chestnut, T. J. (1983). Two-component desensitization at the neuromuscular junction of the frog. *J. Physiol. (Lond.).* 336:229–241.

Damle, V. N., and A. Karlin. 1978. Affinity labeling of one of two $\alpha$-neurotoxin binding sites in acetylcholine receptor from *Torpedo californica. Biochemistry.* 17:2039–2045.

Dunn, S. M., and M. A. Raftery. 1982. Activation and desensitization of *Torpedo* acetylcholine receptor: evidence for separate binding sites. *Proc. Natl. Acad. Sci. USA.* 79:6757–6761.

Feltz, A., and A. Trautmann. 1982. Desensitization at the frog neuromuscular junction: a biphasic process. *J. Physiol. (Lond.).* 322:257–272.

Forman, S. A., L. L. Firestone, and K. W. Miller. 1987. Is agonist self-inhibition at the nicotinic acetylcholine receptor a nonspecific action? *Biochemistry.* 26:2807–2814.

Furchgott, R. F., and P. Bursztyn. 1967. Comparison of dissociation constants and of relative efficacies of selected agonists acting on parasympathetic receptors. *Ann. N.Y. Acad. Sci.* 144:882–899.

Gage, P. W., O. P. Hamill, and R. E. Wachtel. 1983. Sites of action of procaine at the motor end-plate. *J. Physiol. (Lond.).* 335:123–137.

Gurney, A. M., and H. P. Rang. 1984. The channel blocking action of methonium compounds on rat submandibular ganglion cells. *Br. J. Pharmacol.* 82:623–642.

Heidmann, T., and J.-P. Changeux. 1986. Characterization of the transient agonist-triggered state of the acetylcholine receptor rapidly labelled by the noncompetitive blocker [$^3$H]-chlorpromazine: additional evidence for the open channel conformation. *Biochemistry.* 25:6109-6113.

Heidmann, T., J. Bernhardt, E. Neumann and J.-P. Changeux. 1983. Rapid kinetics of agonist binding and permeability response analyzed in parallel on acetylcholine receptor-rich membranes from *Torpedo marmorata. Biochemistry.* 22:5452–5459.

Hess, G. P., E. B. Pasquale, J. W. Walker, and M. G. McNamee. 1982. Comparison of acetylcholine receptor-controlled cation flux in membrane vesicles from *T. californica* and *E. electricus:* chemical kinetic measurements in the millisecond region. *Proc. Natl. Acad. Sci. USA.* 79:963–967.

Hess, G. P., D. J. Cash, and H. Aoshima. 1983. Acetylcholine receptor-controlled ion translocation: chemical kinetic investigations of the mechanism. *Annu. Rev. Biophys. Bioeng.* 12:443–473.

Huganir, R. L., A. H. Delcour, P. Greengard, and G. P. Hess. 1986. Phosphorylation of the nicotinic acetylcholine receptor regulates its rate of desensitization. *Nature (Lond.).* 321:774–776.

Karpen, J. W., A. B. Sachs, D. J. Cash, E. B. Pasquale, and G. P. Hess. 1983. Direct spectrophotometric detection of cation flux in membrane vesicles: stopped-flow measurements of acetylcholine receptor-mediated ion flux. *Anal. Biochem.* 135:83–94.

Katz, B., and S. Thesleff. 1957. A study of the "desensitization" produced by acetylcholine at the motor end-plate. *J. Physiol (Lond.).* 138:63–80.

Lester, H. A., and J. M. Nerbonne. 1982. Physiological and pharmacological manipulations with light flashes. *Annu. Rev. Biophys. Bioeng.* 11:151–175.

Magleby, K. L., and B. S. Pallotta. 1981. A study of desensitization of acetylcholine receptors using nerve-released transmitter in frog. *J. Physiol. (Lond.).* 316:225–250.

Neely, A., and C. J. Lingle. 1986. Trapping of an open channel blocker at the frog neuromuscular junction. *Biophys. J.* 50:981–986.

Neher, E. 1983. The charge carried by single-channel currents of rat cultured muscle cells in the presence of local anesthetics. *J. Physiol (Lond.).* 339:663–678.

Neher, E., and J. H. Steinbach. 1978. Local anesthetics transiently block currents through single acetylcholine receptor channels. *J. Physiol. (Lond.).* 277:153–176.

Neubig, R. R., and J. B. Cohen. 1979. Equilibrium binding of [$^3$H]-tubocurarine and [$^3$H]-ACh by *Torpedo* postsynaptic membranes: stoichiometry and ligand interactions. *Biochemistry.* 18:5465–5475.

Neubig, R. R., and J. B. Cohen. 1980. Permeability control by cholinergic receptors in *Torpedo* postsynaptic membranes: agonist dose-response relationships measured at second and millisecond times. *Biochemistry.* 19:2770–2779.

Neubig, R. R., N. D. Boyd, and J. B. Cohen. 1982. Conformations of *Torpedo* acetylcholine receptor associated with ion transport and desensitization. *Biochemistry.* 21:3460–3467.

Ogden, D. C., and D. Colquhoun. 1985. Ion channel block by acetylcholine, carbachol and suberyldicholine at the frog neuromuscular junction. *Proc. R. Soc. Lond. B.* 225:329–355.

Pasquale, E. B., K. Takeyasu, J. B. Udgaonkar, D. J. Cash, M. C. Severski, and G. P. Hess. 1983. Acetylcholine receptor: evidence for a regulatory binding site in investigations of suberyldicholine-induced transmembrane ion flux in *Electrophorus electricus* membrane vesicles. *Biochemistry.* 22:5967–5973.

Sakmann, B., J. Patlak, and E. Neher. 1980. Single ACh-activated channels show burst kinetics in presence of desensitizing concentrations of agonist. *Nature (Lond.)* 286:71–73.

Shiono, S., K. Takeyasu, J. B. Udgaonkar, A. H. Delcour, N. Fujita, and G. P. Hess. 1984. Regulatory properties of acetylcholine receptor: evidence for two different inhibitory sites, one for acetylcholine and the other for a noncompatetive inhibitor of receptor function (procaine). *Biochemistry,* 23:6889–6893.

Sine, S. M., and J. H. Steinbach. 1984. Agonists block currents through acetylcholine receptor channels. *Biophys. J.* 46:277–284.

Sine, S. M., and P. Taylor. 1980. The relationship between agonist occupation and the permeability response of the cholinergic receptor revealed by bound cobra $\alpha$-toxin. *J. Biol. Chem.* 255:10144–10156.

Takeyasu, K., S. Shiono, J. B. Udgaonkar, N. Fujita, and G. P. Hess. 1986. Acetylcholine receptor: characterization of the voltage dependent regulatory (inhibitory) site for acetylcholine in membrane vesicles from *Torpedo californica* electroplax. *Biochemistry.* 25:1770–1776.

Takeyasu, K., J. B. Udgaonkar, and G. P. Hess. 1983. Acetylcholine receptor: evidence for a voltage-dependent regulatory site for acetylcholine; chemical kinetic measurements in membrane vesicles using a voltage clamp. *Biochemistry.* 22:5973–5978.

Udgaonkar, J. B., and G. P. Hess. 1986. Acetylcholine receptor: chemical kinetics. *J. Membr. Biol.* 93:93–109.

Walker, J. W., M. G. McNamee, E. Pasquale, D. J. Cash, and G. P. Hess. 1981. Acetylcholine receptor inactivation in *Torpedo californica* electroplax membrane vesicles: detection of two processes in the millisecond time region. *Biochem. Biophys. Res. Commun.* 100:86–90.

Walker, J. W., K. Takeyasu, and M. G. McNamee. 1982. Activation and inactivation kinetics of *Torpedo californica* acetylcholine receptor in reconstituted membranes. *Biochemistry.* 21:5384–5389.

Wolosin, J. M., A. Lydiatt, J. O. Dolly, and E. A. Barnard. 1980. Stoichiometry of the ligand-binding sites in the acetylcholine-receptor oligomer from muscle and from electric organ. *Eur. J. Biochem.* 109:495–505.